Statistical giant dipole resonance decay of highly excited states of ^{63}Cu

M. Kicińska-Habior,* K. A. Snover, C. A. Gossett, J. A. Behr, G. Feldman, H. K. Glatzel, and J. H. Gundlach
Nuclear Physics Laboratory, University of Washington, Seattle, Washington 98195

E. F. Garman
Nuclear Physics Laboratory, University of Oxford, Oxford, United Kingdom
(Received 27 April 1987)

Continuum γ-ray spectra from decays of ^{63}Cu formed at initial excitation energies of 22.5 to 77.4 MeV and maximum spin up to $40\hbar$, using ^{4}He+^{59}Co, ^{6}Li+^{57}Fe, ^{12}C+^{51}V, and ^{18}O+^{45}Sc entrance channels, have been measured and analyzed. The parameters of the giant dipole resonance strength function have been extracted using a statistical code in a nonlinear least-squares fitting routine. Except for the cases of ^{4}He and ^{6}Li at the highest bombarding energies, which show evidence for nonstatistical effects, spectra are well reproduced by statistical calculations. The mean energy and strength of the giant dipole resonance built on excited states of ^{63}Cu are close to the ground-state values, while the width varies smoothly from $\sim$5 MeV for the ground-state giant dipole resonance up to 10.6$\pm$0.6 MeV in the temperature range up to 1.9 MeV and mean spin in the range 0–23$\hbar$. The large range of energies studied permitted different level density formulations to be tested. Measured spectra from ^{6}Li+^{98}Mo and ^{6}Li+^{181}Ta at $E_{lab}(^{6}\text{Li})=36$ MeV show a strong nonstatistical enhancement at high γ-ray energies.

I. INTRODUCTION

During the last few years, strong evidence for the existence of the isovector giant dipole resonance (GDR) in hot nuclei has been found in γ-ray spectra associated with heavy-ion fusion reactions.[1–11] Nevertheless, very little experimental information is available on the dependence of statistical GDR decay parameters as functions of temperature and spin in a given nucleus.[2,5,8,11] In a recent paper, Gaardhøje *et al.*[11] have reported a large increase of the GDR width in ^{108,111}Sn* nuclei with increasing nuclear temperature and angular momentum.

On the theoretical side, a number of investigations into the temperature and spin dependence of collective states in a hot nucleus have been reported recently.[12–20] It was found that the temperature dependence of the giant dipole resonance energy should be very weak in the temperature range from $T=0$ to 2 MeV.[12,14,17] Similar results were obtained for the angular momentum dependence of the GDR energy at fixed temperature.[14,20] Also, the strength of the GDR is expected to be nearly independent of temperature.[17] The width of the GDR, however, should increase at higher temperature due to thermal averaging over a distribution of deformations.[19]

In this paper, we examine the GDR decay of the equilibrated hot nucleus ^{63}Cu*, to investigate the possible dependence of the GDR energy, width, and strength on the nuclear temperature and spin. The shape of the GDR built on the ground state of ^{63}Cu has been measured in photoneutron reactions[21–24] and has been described adequately by a double Lorentzian with peak energies E_j, widths Γ_j and strengths S_j (in units of the classical dipole sum rule) of $E_1=16.7$ MeV, $\Gamma_1=4.2$ MeV, $E_2=19.1$ MeV, $\Gamma_2=3.6$ MeV, and $S_2/S_1\cong 0.5$[23] or $E_1=16.2$ MeV, $\Gamma_1=4.7$ MeV, $E_2=19.7$ MeV, $\Gamma_2=4.6$ MeV, and $S_2/S_1\cong 0.4$.[25] Although the observed broadening of the (γ,n) excitation curve has previously been attributed to deformation splitting,[24,25] it has a more natural explanation in terms of the isospin splitting of the GDR into two components, one with $T_<=T_3$ and the other with $T_>=T_3+1$. Isospin splitting of the GDR has been observed in other nuclei near mass $A\sim 60$.[26–29] The magnitude of this splitting[30] is related to the nuclear symmetry energy, and for ^{63}Cu it is estimated to be 3.3 MeV, in agreement with the observed shape of the (γ,n) excitation curve.[21–24] The calculated strength ratio[31] S_2/S_1 due to isospin splitting is 0.3. This is in reasonable agreement with experiment, given that the splitting is not resolved and hence S_2/S_1 is not well defined experimentally. The mean GDR energy calculated from the parameters of the double Lorentzian corresponds to 17.4 MeV, and the $T_<$ and $T_>$ components are expected at 16.7 and 20.0 MeV, respectively, based on the calculated energy splitting and strength ratio given above. There are no available experimental data from photoproton reactions on ^{63}Cu, but in neighboring nuclei, ^{60}Ni (Refs. 28 and 29) and ^{64}Zn (Refs. 26 and 27), both the $T_<$ and $T_>$ components of the GDR have been observed in (γ,n) and (γ,p) excitation curves. To estimate the fraction of the classical dipole sum rule exhausted by the GDR built on the ground state, the (γ,p) cross section has to be taken into account. For ^{63}Cu the (γ,p) cross section was estimated from evaporation theory to be 21% of the total integrated cross section, which, together with the measured (γ,n) cross section, corresponds to a total GDR strength of $S\cong 0.97$.[21] This estimated value of the (γ,p) cross section is in agreement with measured values for the neighboring nuclei Cu[65] (Ref. 32) and ^{64}Zn (Ref. 27).

In order to produce the ^{63}Cu compound nucleus over a large range of excitation energies and spins, and also to populate it at the same excitation energy but with

TABLE I. Characteristics of the ^{63}Cu* states populated in the present work.

Entrance channel	Q value (MeV)	V_{Coulomb}[a] (MeV)	E_{lab}[b] (MeV)	E_{xi} (MeV)	I_i[c] ($\hbar$)
^{18}O+^{45}Sc	23.73	34.0	75.1	77.4	23.0
			53.1	61.6	15.5
			39.9	52.2	8.5
^{12}C+^{51}V	13.38	24.8	64.7	65.7	20.0
			48.0	52.2	15.5
			32.2	39.5	8.5
			26.3	34.7	3.0
^{6}Li+^{57}Fe	19.48	12.3	36.0	52.0	11.5
			22.1	39.5	7.0
			13.9	32.0	2.0
^{4}He+^{59}Co	5.77	8.6	28.4	32.4	5.5[d]
			23.9	28.1	7.5
			17.8	22.5	4.5

[a]In the lab system.
[b]E_{lab} averaged over the target thickness.
[c]Estimated as $2l_0/3$.
[d]It is not clear why such a small value of l_0 is needed in this case to reproduce the low-energy part of the spectrum.

different initial spin distributions, we studied different reaction entrance channels using ^{18}O, ^{12}C, ^{6}Li, and ^{4}He projectiles. In these reactions, only the $T_<$ component of the GDR is populated. The characteristics of the ^{63}Cu compound nucleus formed in these four reactions are presented in Table I. For the cases studied, the initial excitation energy E_{xi} varies from 22.5 to 77.4 MeV, whereas the average initial spin I_i changes from $2\hbar$ to $23\hbar$, corresponding to a total range of initial angular momentum up to about $40\hbar$.

II. EXPERIMENTAL PROCEDURE AND DATA ANALYSIS

The experiments were performed using ^{18}O, ^{12}C, ^{6}Li, and ^{4}He beams produced by the University of Washington FN tandem Van de Graaf accelerator. Self-supporting rolled metallic targets of 99.9% chemical purity were produced from natural material for ^{45}Sc, ^{51}V, and ^{59}Co, and from ^{57}Fe isotopically enriched to 90–95 %. The target thicknesses, determined to ±5% by measuring the energy loss of 5.486 MeV α particles from an ^{241}Am source, were found to be 1.1, 1.0, 4.2, and 1.5 mg/cm^2 for ^{45}Sc, ^{51}V, ^{57}Fe, and ^{59}Co, respectively.

Gamma rays from the decay of ^{63}Cu* were detected at a lab angle of 90° with respect to the beam axis, in a 25.4 cm×25.4 cm NaI(Tl) crystal surrounded by a plastic anticoincidence shield,[33] passive ^{6}LiH and Pb shielding, and with a 40 cm thick paraffin block between the detector assembly and the target. Pulsed beams and time-of-flight techniques with 3.5 ns time resolution over a 1 m flight path were used to separate prompt γ rays produced in the target from neutron-induced events. Cosmic-ray events were rejected by an anticoincidence condition with pulses from the plastic shield. Data were collected with a low spectrum threshold ($E_\gamma \cong 3$ MeV) and at counting rates of 10–15 kHz (above 0.25 MeV), making a pileup correction necessary. A fast pileup rejection circuit with a measured efficiency of 50% was used. The spectrum of pileup-rejected events was recorded, and an additional off-line subtraction was performed in order to completely remove pileup from the γ-ray spectra. The efficiency of the rejection circuit and the validity of the resubtraction technique were determined from measurements made at different beam currents. Pileup was most severe in our spectra in the "knee" region $E_\gamma \sim 10$–13 MeV, but even here the pileup correction was less than 2% for all spectra. The gain stability of the spectrometer was better than 0.2% over long (6 d) runs owing to the combined active transistor-stabilized bases and light-emitting-diode stabilization system.[34] The detector energy resolution was about 4% at 22.6 MeV. The absolute gain calibration was determined using peaks in the range $E_\gamma = 2$–22.6 MeV from p+^{11}B reactions for $E_p = 7.25$ MeV and typically was checked at the beginning and end of each running period. Such a procedure was necessary because the gain must be known accurately at high E_γ, where the heavy-ion-induced spectra are smooth and featureless.

A small but significant background from light target impurities was present in the γ-ray spectra. Additional measurements with ^{18}O or ^{12}C beams at projectile energies below the Coulomb barrier for the target nuclei, but well above the barrier for light nuclei, demonstrated that the background was due to carbon and oxygen target impurities. From these measurements the amount of carbon and oxygen impurities in the targets of interest was determined. Background spectra from carbon and oxygen targets, the latter obtained from difference spectra measured with Ta_2O_5 and Ta targets, were measured at all relevant bombarding energies and used to correct the spectra of interest. This background subtraction mainly affected the low-energy part of the γ-ray spectra

($E_\gamma < 10$ MeV); in the energy range of primary interest ($E_\gamma > 10$ MeV), background corrections were less than 2%.

Absolute cross sections at 90° were obtained to ±10% by direct calculation from the measured γ-ray yields after correcting for pileup, deadtime, and light contaminants. The calculations were based on knowledge of target thickness, total accumulated charge, solid angle, and γ-ray detection efficiency of the NaI crystal. Total cross sections were obtained assuming an isotropic angular distribution. For data taken with the ^{57}Fe target, no correction was applied for the 5–10% ^{56}Fe in the target; however, statistical model calculations showed that the cross section as well as the fitted GDR parameters were completely insensitive to this impurity.

The γ-ray detector efficiency is based on direct measurement for energies between 2.3 and 15.1 MeV; for higher energies, an extrapolation has been made consistent with an EGS (electron gamma shower) Monte Carlo calculation. For the present energies of interest, the efficiency is known to approximately ±5%. Because the detector response to monenergetic photons involves a "photopeak" plus a low-energy tail, the raw data cannot be converted to cross section without deconvoluting the response function. Instead, we convolute the statistical model calculation with the measured detector response (energy-dependent line shape and efficiency) and compare directly with the data, as shown in Figs. 1, 6, 7, 9, and 10. The vertical scale in these figures has been determined by the detector efficiency at $E_\gamma = 15.1$

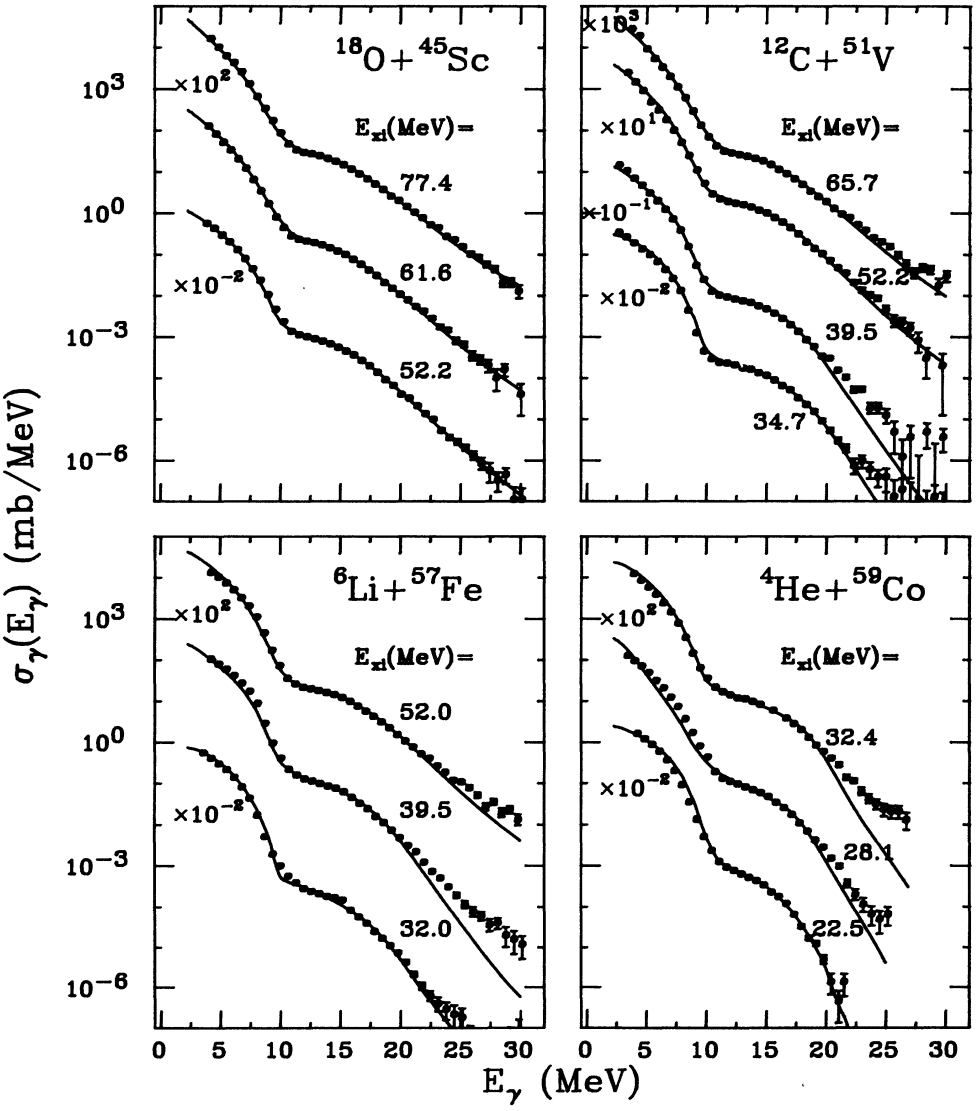

FIG. 1. Measured γ-ray spectra from the decay of ^{63}Cu* together with least-squares-fitted statistical model calculations for the level density parameters in the Pühlhofer approach: $a_{\mathrm{LDM}} = A/8$ MeV^{-1} and Δ_{LDM} calculated from the Myers droplet model formula without the Wigner term.

MeV, and because the efficiency variation with energy is slow, this scale is correct to within 10% for $E_\gamma = 5-20$ MeV.

III. RESULTS

Gamma-ray spectra from the decay of the compound nucleus ^{63}Cu* formed at different initial excitation energies and initial spins are presented in Fig. 1. All these spectra show the same qualitative shape: a relatively intense yield of low-energy γ rays ($E_\gamma < 10$ MeV) emitted after the compound nucleus has cooled by particle evaporation to near particle threshold, and a high-energy part with the characteristic broad bump, arising from γ-ray emission in direct competition with particle evaporation. The solid curves represent statistical model calculations which are described in Sec. III B.

Figure 2 displays the experimental spectra from the decay of ^{63}Cu* compound nuclei populated at the same excitation energy ($E_{xi} = 52.5$ MeV) but with different initial spin distributions produced by ^{18}O+^{45}Sc, ^{12}C+^{51}V, and ^{6}Li+^{57}Fe entrance channels. The spectral shapes are very similar for the ^{18}O and ^{12}C channels, in agreement with the hypothesis that compound nuclear decays should be independent of the entrance channel. Small discrepancies for the ^{6}Li channel compared with the ^{18}O and ^{12}C channels at the highest γ-ray energies are due to a nonstatistical enhancement of the γ-ray emission[6,10] in the ^{6}Li channel (see Sec. III C).

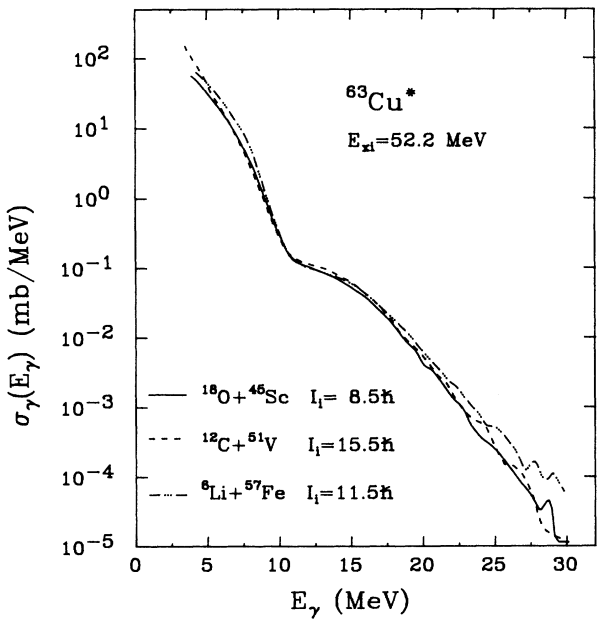

FIG. 2. Experimental γ-ray spectra from the decay of ^{63}Cu* formed at $E_{xi} = 52.2$ MeV with different spin distributions produced by different reaction entrance channels: ^{18}O+^{45}Sc, ^{12}C+^{51}V, and ^{6}Li+^{57}Fe. In order to compare the high-energy spectral shapes, the latter two spectra were normalized near $E_\gamma = 10-12$ MeV by factors of 0.62 and 0.47, respectively, to match the ^{18}O+^{45}Sc spectrum.

A. Statistical model analysis

Gamma-ray cross sections were calculated using a modified version of the computer code CASCADE,[35] which is based on the assumption that the heavy-ion fusion reaction forms a highly excited compound nucleus in thermal equilibrium. The decay width for emitting a γ ray of energy E_γ was assumed to have the form

$$\frac{d\Gamma_{\gamma L}(E_\gamma, I_i \rightarrow I_f)}{dE_\gamma} = \frac{\rho(E_f, I_f, \pi_f)}{\rho(E_i, I_i, \pi_i)} \frac{E_\gamma^2}{(\pi\hbar c)^2} \frac{\sigma_{\rm abs}^{EL}(E_\gamma)}{2L+1} , \quad (1)$$

where $E_\gamma = E_i - E_f$, ρ is the level density discussed in Sec. III B, L denotes the multipolarity of the γ ray, and $\sigma_{\rm abs}^{EL}(E_\gamma)$ represents the cross section for EL photoexcitation.

In our calculations the averaged absorption cross section for electric dipole radiation was represented by a Lorentzian form with peak energy E_D, width Γ, and strength S (in units of the classical dipole sum rule) characterizing the giant dipole resonance:

$$\sigma_{\rm abs}^{E1}(E_\gamma) = \frac{4\pi e^2\hbar}{Mc} \frac{NZ}{A} \frac{S E_\gamma^2 \Gamma}{(E_D^2 - E_\gamma^2)^2 + E_\gamma^2 \Gamma^2} . \quad (2)$$

The parameters of the GDR (E_D, Γ, and S) were treated as variables in the least-squares fitting of the calculated spectra to the experimental data. For $E2$ transitions, both isovector (IVGQR) and isoscalar (ISGQR) giant quadrupole resonance components were included with fixed parameters $E = 15.8$ MeV, $\Gamma = 4.0$ MeV, and $S = 1.0$ for the ISGQR, and $E = 31.4$ MeV, $\Gamma = 5.0$ MeV, and $S = 1.0$ for the IVGQR. The contribution of the GQR in the analyzed spectra was small ($< 5\%$ for $E_\gamma < 20$ MeV, $\sim 8\%$ for $E_\gamma = 25$ MeV), and the calculated spectrum shapes were insensitive to changes of GQR parameters (e.g., using parameters from Kawazoe *et al.*[36]). The biggest effect from $E2$ is at the highest projectile energies for ^{18}O+^{45}Sc at $E_{xi} = 77.4$ MeV, where the IVGQR contributes $\sim 30\%$ of the yield at $E_\gamma \cong 30$ MeV and the statistical model calculation appears slightly worse compared to the data if the IVGQR contribution is omitted.

The spectrum shape calculated using CASCADE is the sum of γ-ray spectra from the decay of the initial compound nucleus and the daughter nuclei populated by particle emission. Figure 3(a) shows a calculated decomposition into individual components of the spectrum of γ rays from ^{12}C+^{51}V$\rightarrow$^{63}Cu* at $E_{xi} = 52.2$ MeV. In Fig. 3(b) a representative particle decay chain for the same reaction as in Fig. 3(a) is displayed. It can be seen from Fig. 3(b) that low-energy γ rays are emitted mainly after sequential particle decays. High-energy γ decay is predominantly due to γ-ray emission from the initial compound nucleus, and the ranges of final spin and energy populated are indicated for this component by the dotted lines in Fig. 3(b). It is evident from Fig. 3(a) that at high γ-ray energies the γ decay of the initial compound nucleus dominates, but that γ decay following emission of one particle is also important.

All calculated spectra were folded with the measured energy-dependent response function of the detector for comparison with the data. In the case of the ^{4}He+^{59}Co

channel, the calculated spectra were normalized to agree at low γ-ray energy with the measured spectra, by varying the grazing angular momentum l_0. All other spectra calculated with the fusion cross section as given by CASCADE agreed with the measured spectra at low E_γ. The experimental data were fitted over the region $E_\gamma \geq 12$ MeV, where the spectrum shape is most sensitive to the GDR parameters.

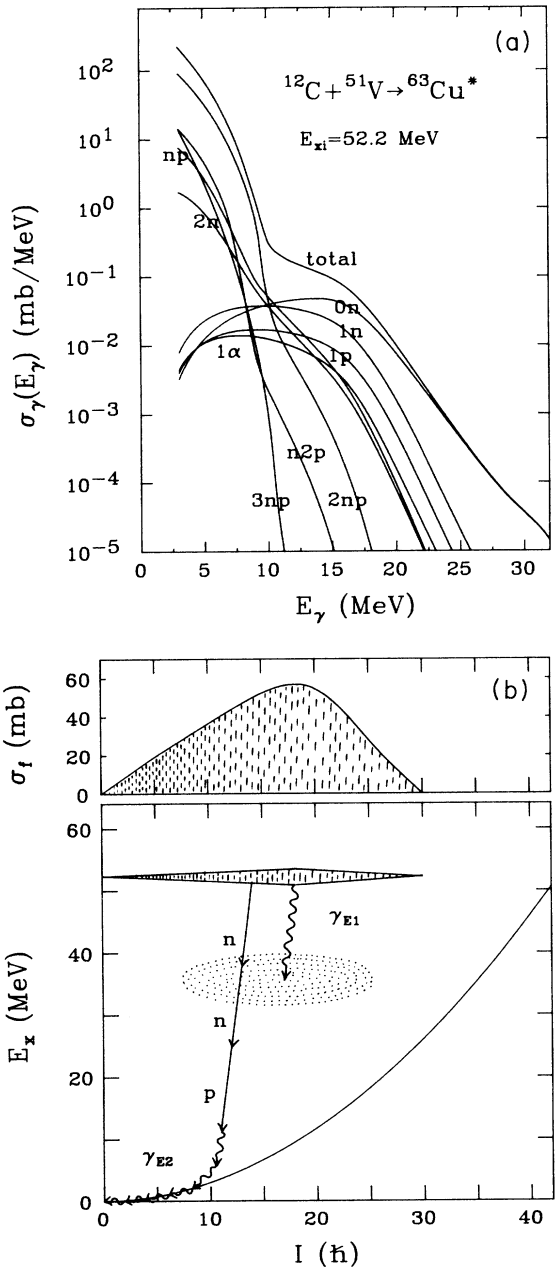

FIG. 3. CASCADE statistical model calculations of γ decay from $^{12}C+^{51}V\rightarrow^{63}Cu^*$ for $E_{xi}=52.2$ MeV (without line shape folding). (a) Total spectrum, γ decay from the initial compound nucleus (labeled 0n) and γ decay following emission of the labeled particle. (b) Calculated initial spin distribution σ_f, yrast line, a representative particle decay chain, and the most probable high-energy γ-ray decay. The outer contour shown for γ decay corresponds roughly to the half-width of the intensity distribution as a function of spin and energy.

B. Level density

The level density of the initial compound nucleus and its daughters is a quantity of primary importance in the CASCADE calculations. Although the nuclear level density has been studied for many years, there are still unresolved uncertainties concerning it.[37] Several semiempirical formulae have been proposed and used in statistical model calculations. In the present study, many γ-ray spectra over a wide range of excitation energy were measured, giving us a unique opportunity for testing level density formulations in a self-consistent manner.

We have investigated three different formulations: (1) the original CASCADE level density approach proposed by Pühlhofer[35] in which the level density is defined separately in different regions of excitation energy; (2) variations on the Pühlhofer approach; (3) the approach suggested by Reisdorf[44] in which the level density at all excitation energies is given by one smoothly varying formula. Our criteria in determining the acceptability of the level density description were that it should result in good fits of the statistical calculations to the experimental data over a wide range of excitation energies, that the extracted GDR parameters should vary smoothly with excitation energy and spin, and that the calculated level densities should agree with values determined experimentally from direct level counting, high resolution (p,p) resonance measurements, and Ericson fluctuation measurements.[41]

1. The Pühlhofer approach and variations

As a large range of excitation energies is important in the decay of a highly excited nucleus [as seen in Fig. 3(b) for $^{63}Cu^*$], it was proposed by Pühlhofer[35] that the level density should be defined separately in four regions. At "low" excitation energy (typically $E_x \leq 5$ MeV), individual levels for the initial compound nucleus and for each daughter nucleus should be taken into account. In the case of $^{63}Cu^*$ and its daughters, individual levels are known experimentally up to about 3.5 MeV in excitation energy. At higher excitation, where the energies and spins of individual levels are unknown, the functional form of the level density for a given angular momentum I and both parities together as a function of excitation energy E is given by

$$\rho(E,I)=\frac{2I+1}{12\theta^{3/2}}\sqrt{a}\,\frac{\exp(2\sqrt{aU})}{(U+t)^2}\ , \tag{3}$$

where

$$U=E-\Delta-I(I+1)/\theta'=at^2-t\ ,$$

$$\theta=2J_{\text{rigid}}/\hbar^2\ ,$$

and

$$\theta'=\theta(1+\delta I^2+\delta' I^4)\ .$$

Here, t is the nuclear temperature, J_{rigid} is the rigid-body moment of inertia $J_{\text{rigid}}=2mR^2/5$ with $R=r_0A^{1/3}$, and θ' represents the moment of inertia of a deformable rotating liquid drop with small deformability coefficients δ and δ'. The parameters a and Δ are defined separately in different regions of excitation energy. For "medium" energies, in the range $3.5\ \text{MeV}<E_x<40/A^{1/3}$ MeV$=10.1$ MeV for ^{63}Cu, the level density was calculated according to (3) with the empirically determined parameters a and Δ taken from the compilation of Dilg *et al.*[38] where available, and where unavailable an analytic formula[38] approximating the mass dependence and shell effects on a and Δ was applied. To specify the spin dependence of the level density in this region, we used the parameter $r_0=1.17$ fm corresponding to an effective moment of inertia of 85% of the rigid-body value, as suggested by Pühlhofer,[35] in order to continue smoothly the yrast line above the known high-spin states.

At "high" energies, above $E_x>80/A^{1/3}$ MeV$=20.1$ MeV for ^{63}Cu, where shell and pairing effects are assumed to have vanished, the smooth mass dependence for a and Δ given by the liquid drop model was assumed. The generally accepted values of $a_{\text{LDM}}=A/8\ \text{MeV}^{-1}$, and Δ_{LDM} defined as the difference between the experimental and the liquid drop binding energy calculated from the Myers droplet model mass formula[39] without shell and pairing corrections, were used. Yrast line parameters $r_{0_{\text{LDM}}}=1.27$ fm,[40] $\delta=3.9\times10^{-5}$, and $\delta'=3.5\times10^{-8}$ were chosen according to the prescription given by Pühlhofer.[35] In the transition region between the "medium" and "high" energies, $40/A^{1/3}\ \text{MeV}\le E_x\le 80/A^{1/3}$ MeV, a linear interpolation of a, Δ, and θ was performed.[35]

The best fits of the CASCADE calculations to the experimental data using the level density formulation given above are shown in Fig. 1 by solid lines. The γ-ray spectra from the decay of the highly excited ^{63}Cu* compound nucleus formed at initial energies $E_{xi}\ge 52$ MeV in ^{18}O$+^{45}$Sc and ^{12}C$+^{51}$V reactions are very well reproduced by these calculations. At the lower initial excitation energies ($E_{xi}<40$ MeV), however, some discrepancies occur. The calculations underestimate the measured γ-ray yield for $E_\gamma>20$ MeV, as can be seen in Fig. 1. The γ-ray spectra observed from the ^{12}C$+^{51}$V and ^{6}Li$+^{57}$Fe channels at $E_{xi}<40$ MeV cannot be fitted by CASCADE calculations with the level density parameter $a_{\text{LDM}}=A/8\ \text{MeV}^{-1}$ and the value of Δ_{LDM} calculated from the Myers droplet model mass formula.[39] For the highest projectile energies in the ^{6}Li$+^{57}$Fe and ^{4}He$+^{59}$Co channels, the measured γ-ray yield is also larger than the calculated yield; here, however, nonstatistical reaction contributions have to be taken into account (see Sec. III C). For moderate projectile energies, the ^{18}O$+^{45}$Sc and ^{12}C$+^{51}$V channels are well described by the statistical model, and so we have to look for another explanation for the observed discrepancies. We will focus on the data from the ^{12}C$+^{51}$V reaction at $E_{xi}=39.5$ MeV, as the most obvious discrepancy occurs for this case.

We examined the possibility that the discrepancies between the normal statistical calculations and our data for low projectile energies might be due to an error in the assumed initial spin distribution. In our calculations, the initial spin distributions were calculated using the strong absorption model with the transmission coefficients approximated by a Fermi distribution with a diffuseness $d=2$ fm. This approximation is rather good for strongly absorbed heavy ions, with energies well above the Coulomb barrier. For incident projectile energies near and below the Coulomb barrier, however, a broader spin distribution for the resulting compound nucleus is expected.[42] In order to investigate the sensitivity of the calculated spectrum shape to a change in the initial spin distribution, we have fitted the γ-ray spectrum for the ^{12}C$+^{51}$V reaction at the lowest two ^{12}C energies, $E_{\text{lab}}=26.3$ and 32.2 MeV, assuming a broader spin distribution. First, we changed the diffuseness of the spin distribution in the range $2\hbar$–$6\hbar$. This required a compensating change in l_0 to keep the fusion cross section constant and to preserve the agreement with the low-energy part of the γ-ray spectrum. Increasing the diffuseness up to $6\hbar$ increased the fitted GDR strength by 15%, while E_D and Γ changed by less than 2%. We also tried a very broad spin distribution as determined by Gil *et al.*[42] for the ^{16}O$+^{154}$Sm reaction at a projectile energy below the Coulomb barrier ($E_{\text{lab}}=63$ MeV), with the fusion cross section normalized to give agreement with the low-energy part of the γ-ray spectrum. In all these cases the calculated spectrum shape remained almost unchanged from the shape calculated with the default spin distribution, thus demonstrating that the observed discrepancies are not due to an error in the initial spin distribution.

On the other hand, it is also possible that the discrepancies between our data and CASCADE calculations can be attributed to an incorrect prescription for the level densities. This was thoroughly investigated, and we show in the following that it can account for our observations. We found that the discrepancies in the fitted spectral shapes are especially sensitive to the dependence of the level density on excitation energy, in particular to the properties of the transition region. We assumed that the parameters a and Δ describing the level density are well defined in the "medium" energy region, where they are extracted from fits to the experimental data.[38] At higher energies the level density parameters are less certain. Especially in the transition region, where shell effects gradually vanish, the linear interpolation of parameters a and Δ is rather arbitrary. In the "high" energy region, the generally accepted value for a_{LDM} is $A/8\ \text{MeV}^{-1}$, but also lower values have been proposed. In order to test the sensitivity of the CASCADE fitting calculations to the parameters describing the level density at higher excitation energies, we performed a series of CASCADE fits to the measured γ-ray spectra using different sets of parameters a_{LDM} and Δ_{LDM} as well as changing the transition region starting point and range. We varied the value of the parameter a_{LDM} from $A/7$ to $A/10\ \text{MeV}^{-1}$ and used Δ_{LDM} calculated from the Myers droplet model mass formula without or with the Wigner term.[39] The Wigner term represents a bulk property of the nucleus, connected

TABLE II. Dependence of GDR parameters on the level density parameters for $^{12}C+^{51}V \rightarrow ^{63}Cu^*$ at $E_{xi}=39.5$ MeV. M, calculated from the Myers droplet model mass formula without the Wigner term; M + Wt, same as M, but with the Wigner term included.

Set	Trans. region (MeV)	A/a_{LDM} (MeV)	Δ_{LDM}	χ^2	S	E_D (MeV)	Γ (MeV)
A	10.1–20.1	8.0	M	6.7	0.98±0.02	16.9±0.1	6.6±0.1
B	10.1–20.1	8.0	M+Wt	5.2	1.09±0.02	17.1±0.1	6.9±0.1
C	10.0–11.0	8.0	M	2.8	1.05±0.02	17.3±0.1	7.4±0.2
D	80.0–82.0	not relevant		1.8	0.93±0.02	16.6±0.1	7.8±0.1
E	10.1–20.1	9.0	M+Wt	1.9	1.01±0.02	16.7±0.1	7.8±0.1
F	10.1–20.1	9.5	M	1.8	0.92±0.02	16.5±0.1	7.6±0.1
G	10.1–20.1	9.0	M	2.9	0.95±0.02	16.6±0.1	7.3±0.1
H	20.0–30.0	8.0	M	9.7	1.43±0.02	17.7±0.1	5.6±0.1

with the increased overlap of the wave functions of particles in identical orbits. The value of the Wigner term is proportional to $N-Z$, and in the case of ^{63}Cu it is significant. The γ-ray spectrum calculated for $^{12}C+^{51}V$ at $E_{xi}=39.5$ MeV was found to be the most sensitive to level density changes. Various sets of level density parameters used in our fits, with corresponding χ^2 values and GDR parameters extracted from fits for this spectrum, are listed in Table II.

We also examined the level density curves calculated for particular sets of parameters a_{LDM} and Δ_{LDM}, and compared them with experimentally determined values of the level density from Lu *et al.*[41] obtained from direct level counting, high resolution (p,p) measurements, and Ericson fluctuation measurements in the energy range up to 24 MeV. Figure 4 shows the level density curves in the excitation energy range up to 24 MeV for ^{63}Cu and for several daughter nuclei calculated using the Pühlhofer approach with the generally accepted $a_{LDM}=A/8$ MeV^{-1} and Δ_{LDM} calculated without the Wigner term (long dashes, marked A), as well as experimentally determined values from Lu *et al.*[41] For comparison, Fig. 4 also displays the level density curves determined by the individual levels at low energy, and by formula (3) with "medium" energy parameters a,Δ,r_0 at all higher energies (dotted curve, marked D). The same curves for ^{63}Cu calculated up to $E_x=70$ MeV are shown in Fig. 5. It is worth emphasizing that the level density

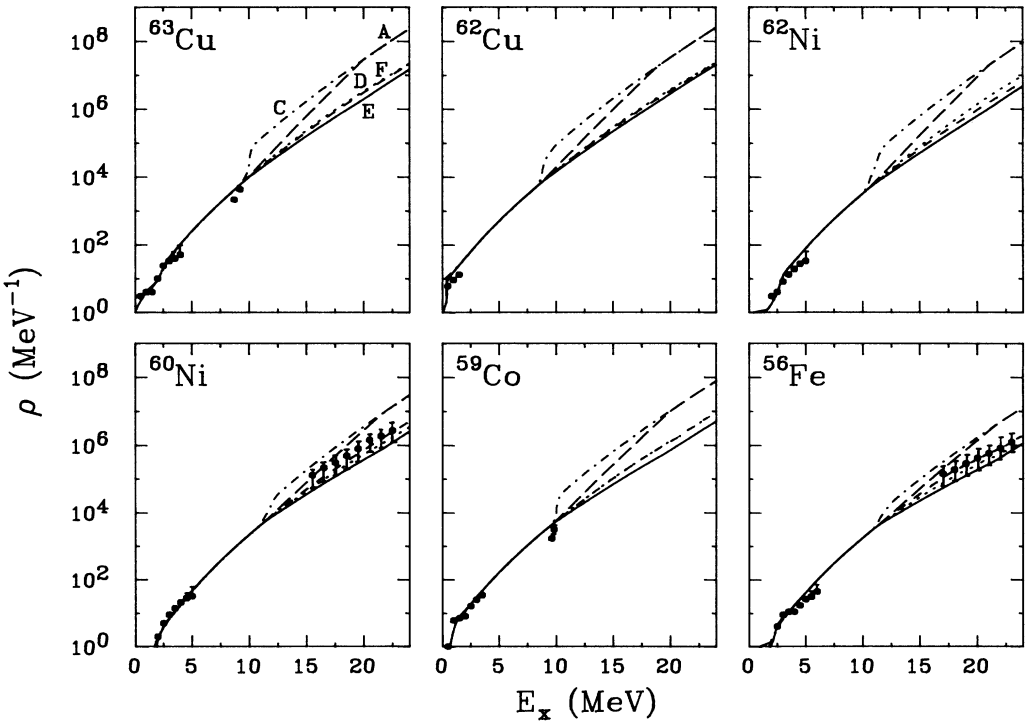

FIG. 4. Level density curves for the initial compound nucleus ^{63}Cu and several daughters, together with the experimental data from Ref. 41. Parameter sets for the level density curves are described in Table II: set A, long dashes; C, dashed-dotted; D, dots; E, solid line; F, short dashes.

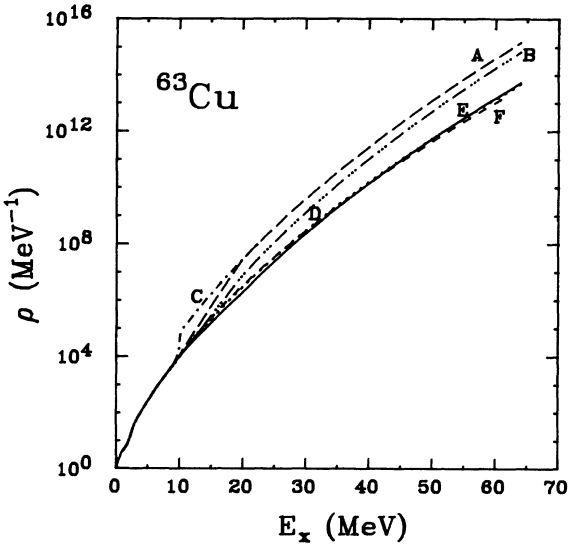

FIG. 5. Level density curves for the ^{63}Cu nucleus calculated for different parameters using the Pühlhofer approach. The definition of the curves is the same as that given in Fig. 4; additional set B, dashed–three-dotted curve (see also Table II).

curve D defined at all energies by the "medium" energy range parameters is very different from A, which is calculated with the generally accepted liquid-drop parameters in the "high" energy region. Curve D has a different slope at high excitation energy, and by definition is a much smoother function in the excitation energy region of 10–20 MeV than the level density *A*, which has obvious slope discontinuities at the ends of the transition region. The experimentally measured level density data agree better with curve D than with curve A (see Fig. 4). The use of level density *D* results in good CASCADE fits to the measured γ-ray spectra for all of the cases which we studied. Extrapolation up to $E_x = 70$ MeV of the "medium" energy parameters, containing the shell effects, seems, however, not to be well motivated. So, we decided to look for a level density curve which has a similar energy dependence, but which is described by a parameter $a_{\rm LDM} = A/\text{const}$ and by a value for $\Delta_{\rm LDM}$ which cancels shell and pairing effects in the "high" energy region, as predicted by the liquid drop model. Such curves for ^{63}Cu and its daughter nuclei can be obtained with $a_{\rm LDM} = A/9$ MeV^{-1} and $\Delta_{\rm LDM}$ calculated from the Myers droplet mass formula with the Wigner term included (solid line in Figs. 4 and 5, marked E) or with $a_{\rm LDM} = A/9.5$ MeV^{-1} and $\Delta_{\rm LDM}$ calculated without the Wigner term (short dashes in Figs. 4 and 5, marked F). These two sets of parameters $a_{\rm LDM}$ and $\Delta_{\rm LDM}$ resulted in the best fits to the data for all excitation energies. The best fits for $a_{\rm LDM} = A/9$ MeV^{-1} and $\Delta_{\rm LDM}$ calculated with the Wigner term are presented in Fig. 6 by solid lines.

The change in the quality of the best CASCADE fit to the measured spectrum shape with the variation of the level density parameters may be judged by comparison of the dashed and solid curves in Fig. 7, corresponding, respectively, to the calculation using $a_{\rm LDM} = A/8$ MeV^{-1} and $\Delta_{\rm LDM}$ calculated without the Wigner term, and $a_{\rm LDM} = A/9$ MeV^{-1} and $\Delta_{\rm LDM}$ calculated with the Wigner term included. In Fig. 7(b) the measured and fitted spectra have been multiplied by the factor $\exp(\alpha E_\gamma)$ in order to approximately cancel the effect of rapidly varying level density with energy and to facilitate comparison of the fitted spectrum and data on a linear scale.

We have also investigated changing the transition region starting point and range in the level density description. However, this only improved the fit quality in the unphysical situation in which the transition region was very low in excitation energy and had a very short range ($E_x = 10$–11 MeV). The corresponding level density curve (dashed-dotted curve in Figs. 4 and 5, marked *C*) does not agree with the experimental values[41] of the level density, and it also has a physically unreasonable slope discontinuity.

Since the yrast lines at high spin in ^{63}Cu and daughter nuclei are not well known, the sensitivity to the parameter r_0 for the "medium" energy region could only be checked by additional CASCADE calculations with different values of r_0. In Table III we present χ^2 values and GDR parameters extracted from fits with three different values of r_0 corresponding to an effective moment of inertia of 50%, 85%, and 100% of the rigid-body value. Although the fitted GDR parameters show some sensitivity to r_0 (see Table III), the fit quality is not changed substantially by altering r_0.

In conclusion, we believe the discrepancies between the CASCADE calculations using the Pühlhofer default level density and measured spectra are caused by an incorrect behavior of the level density at high excitation energies. The default description of the level density has approximately the correct slope at high energies, so that if all high-energy γ decays of interest populate final states which are in the "high" energy region, then statistical decay calculations with this level density produce reasonable results. For such cases, the fit quality is good (see Fig. 1 for $E_{xi} \geq 52$ MeV), and the extracted GDR

TABLE III. Dependence of GDR parameters on the yrast line parameters in the "medium" energy region for $^{12}C + ^{51}V \rightarrow ^{63}Cu^*$ at $E_{xi} = 39.5$ MeV.

Set	r_0 (fm)	Fraction of $J_{\rm rigid}$ (%)	χ^2	S	E_D (MeV)	Γ (MeV)
I	0.90	50	6.9	0.98±0.02	16.9±0.1	6.5±0.1
A	1.17	85	6.7	0.98±0.02	16.9±0.1	6.6±0.1
J	1.27	100	5.0	1.09±0.02	17.1±0.1	7.5±0.2

parameters are in reasonably good agreement with our final results given in Table IV and discussed in Sec. III D—S and Γ within 5% and 2%, respectively, and E_D values systematically higher by about 0.5 MeV. However, if high-energy γ decay populates states in the transition region, then the high-energy γ-ray spectrum is given incorrectly because the level density in the transition region has the wrong slope. This can be seen in Fig. 1 for the cases with $E_{xi}=39.5$ MeV; also, the $E_{xi}=34.7$ and 32.0 MeV fits give physically unreasonable GDR parameters for the same reason. The slope in the transition region is wrong, because the default level density at high energies has too large a magnitude, and hence cannot be matched reasonably with the level density in the "medium" energy region.

The energy dependence of the level density should, of course, be smooth, without unphysical discontinuities. Our analysis shows also that in the Pühlhofer approach the level density parameter $a_{\rm LDM}$ should be in the range $A/9$ to $A/9.5$ MeV^{-1} for nuclei with mass around $A=60$. It can be seen from Fig. 6 that, in general, the fits of the CASCADE calculation with such level density parameters are significantly improved over those in Fig. 1.

2. *The Reisdorf approach*

Recently, another semiempirical level density formula, proposed originally by Ignatyuk *et al.*[43] has been developed independently by Reisdorf,[44] Schmidt *et al.*,[45] and Kataria *et al.*[46] The Reisdorf approach has been followed in the statistical code HIVAP (Refs. 44 and 47) and we will confine our discussion to this approach. It differs from the Pühlhofer approach, mainly by treating

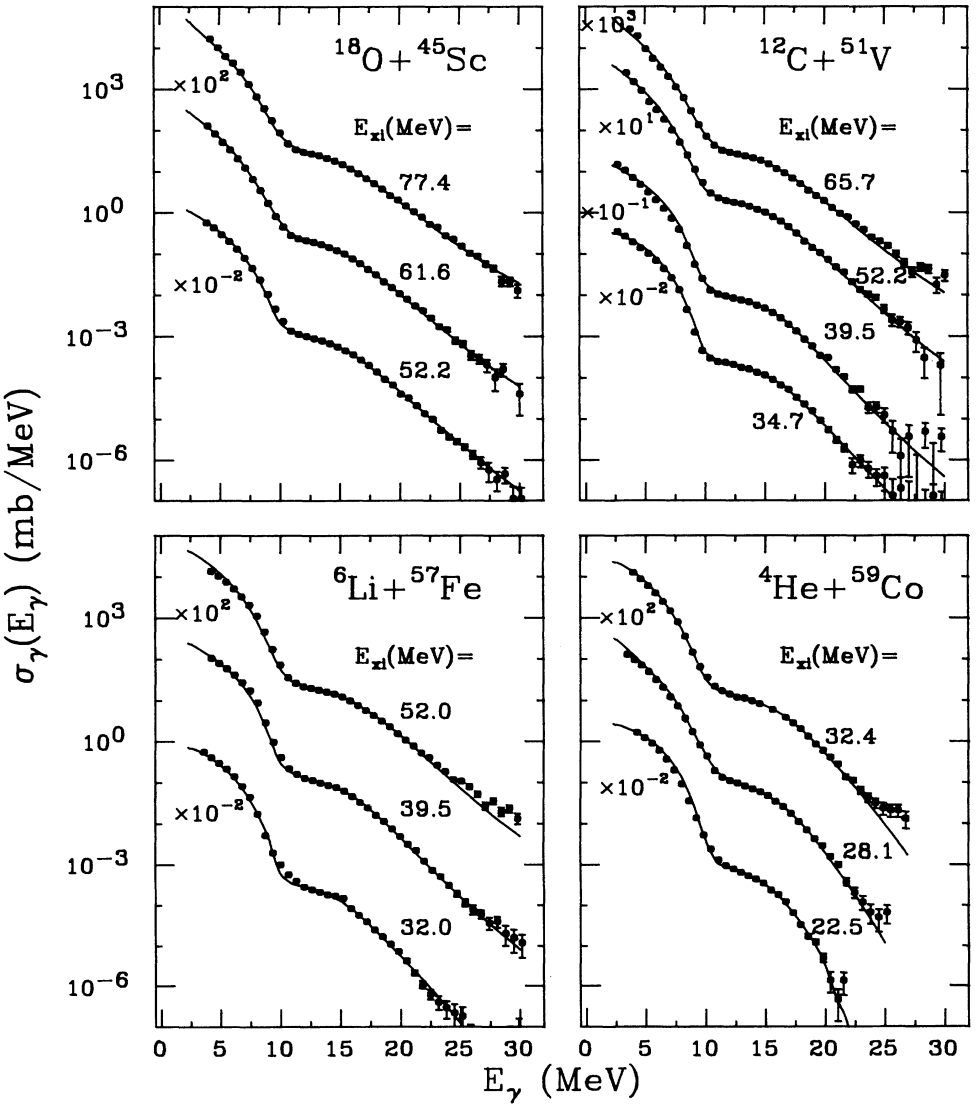

FIG. 6. The same as Fig. 1, but fitted statistical model calculations for the level density parameters: $a_{\rm LDM}=A/9$ MeV^{-1} and $\Delta_{\rm LDM}$ calculated including the Wigner term.

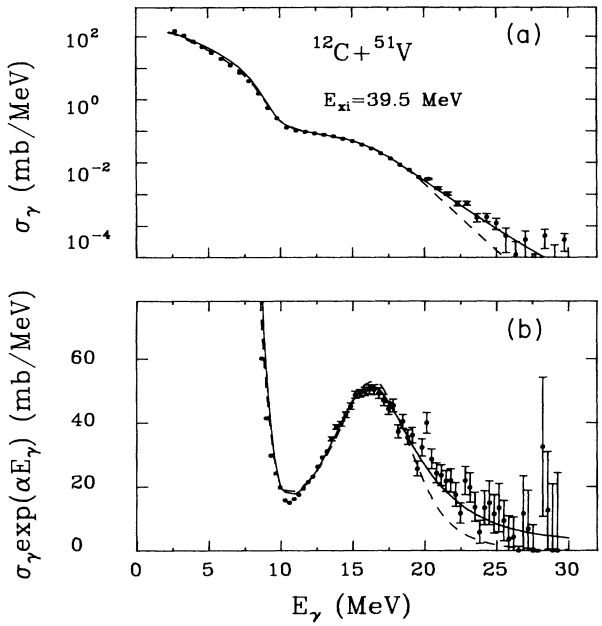

FIG. 7. Comparison of statistical model calculation fits to the data for $^{12}C+^{51}V \rightarrow ^{63}Cu$ at $E_{xi}=39.5$ MeV with different level density parameters. (a) γ-ray spectrum: dashed line for $a_{LDM}=A/8$ MeV^{-1} and solid line for $a_{LDM}=A/9$ MeV^{-1} and Δ_{LDM} calculated using the Wigner term. (b) Measured and calculated γ-ray spectra multiplied by an energy-dependent factor $\exp(\alpha E_\gamma)$, where $\alpha^{-1}=2.2$ MeV, used only to permit convenient comparison of the fit quality on a linear scale.

the level density parameter a as dependent on the ground-state shell correction energy δU and the excitation energy of the nucleus. The level density for angular momentum I and both parities together as a function of excitation energy E is given by

$$\rho(E,I)=\frac{2I+1}{12\theta^{3/2}}\sqrt{a}\,\frac{\exp(2\sqrt{aU})}{U^2}\ , \tag{4}$$

where

$$U=E-I(I+1)/\theta+\delta P\ ,$$

and the energy-dependent parameter a is defined by

$$aU=\tilde{a}[E-I(I+1)/\theta+\delta U+\delta P]-\tilde{a}\delta U\exp(-\gamma U)\ . \tag{5}$$

The pairing correction δP accounts for the odd-even structure in the ground-state masses. $\delta U+\delta P$ is an energy backshift, which cancels the shell and pairing effects at high excitation energies and plays a role similar to $-\Delta$ in the Pühlhofer approach. The smoothly varying level density parameter $\tilde{a}$ is calculated according to a microscopic description[44] containing surface and curvature corrections. For nuclei with mass around $A=60$, $\tilde{a}\approx A/8$ MeV^{-1} (for ^{63}Cu, $\tilde{a}=A/8.17$ MeV^{-1}). The influence of shell effects on the level density is then taken into account by including in the parameter a an additional energy backshift, which decreases exponentially (with a damping factor γ) with increasing excitation energy. In this way, one formula describes the level density over the whole energy range.

For the purpose of our ^{63}Cu decay calculations, we inserted the level density subroutine from the HIVAP code into CASCADE. We have taken the complete expression (4) into account, which was not the case in some other HIVAP calculations.[47] The ground-state shell corrections δU were determined from the differences between the experimental ground-state masses and the liquid drop model predictions.[48] The pairing corrections were calculated in a standard way using the liquid drop model, with odd-mass nuclei chosen as a reference, in which case the pairing correction equals zero for odd A. The obtained

TABLE IV. Extracted parameters of the GDR built on highly excited states of ^{63}Cu*. Values and errors are determined from the average of results obtained with different level densities. The cases ^{6}Li+^{57}Fe (52.0 MeV) and ^{4}He+^{59}Co (32.4 MeV) are contaminated by nonstatistical contributions (see text).

Entrance channel	E_{xi} (MeV)	$\tilde{E}_{xf}$[a] (MeV)	T_f[a] (MeV)	I_f[a] ($\hbar$)	S	E_D (MeV)	Γ (MeV)
^{18}O+^{45}Sc	77.4	29.2	1.93	22.0	0.90±0.10	16.4±0.3	10.6±0.6
	61.6	27.1	1.86	15.0	0.99±0.10	16.3±0.3	9.9±0.5
	52.2	24.6	1.77	8.5	1.10±0.07	16.5±0.4	9.6±0.4
^{12}C+^{51}V	65.7	23.2	1.72	20.5	1.07±0.10	17.0±0.3	10.5±0.5
	52.2	19.2	1.56	16.0	0.87±0.07	16.8±0.3	9.3±0.3
	39.5	16.6	1.45	9.5	0.97±0.05	16.7±0.3	7.7±0.2
	34.7	12.9	1.28	4.5	1.37±0.12	17.1±0.5	8.1±0.6
^{6}Li+^{57}Fe	52.0	23.7	1.73	10.0	0.87±0.07	17.6±0.4	10.2±0.3
	39.5	17.7	1.50	7.5	0.80±0.07	17.1±0.5	8.8±0.3
	32.0	12.0	1.23	3.0	0.74±0.10	16.5±0.6	8.2±0.8
^{4}He+^{59}Co	32.4	11.1	1.19	7.5	2.09±0.20	17.2±1.2	7.9±0.3
	28.1	7.3	0.96	7.8	0.87±0.08	17.4±0.4	7.5±0.4
	22.5	4.3	0.74	5.5	1.25±0.08	17.1±0.1	7.8±0.6

[a]Calculated as described in text.

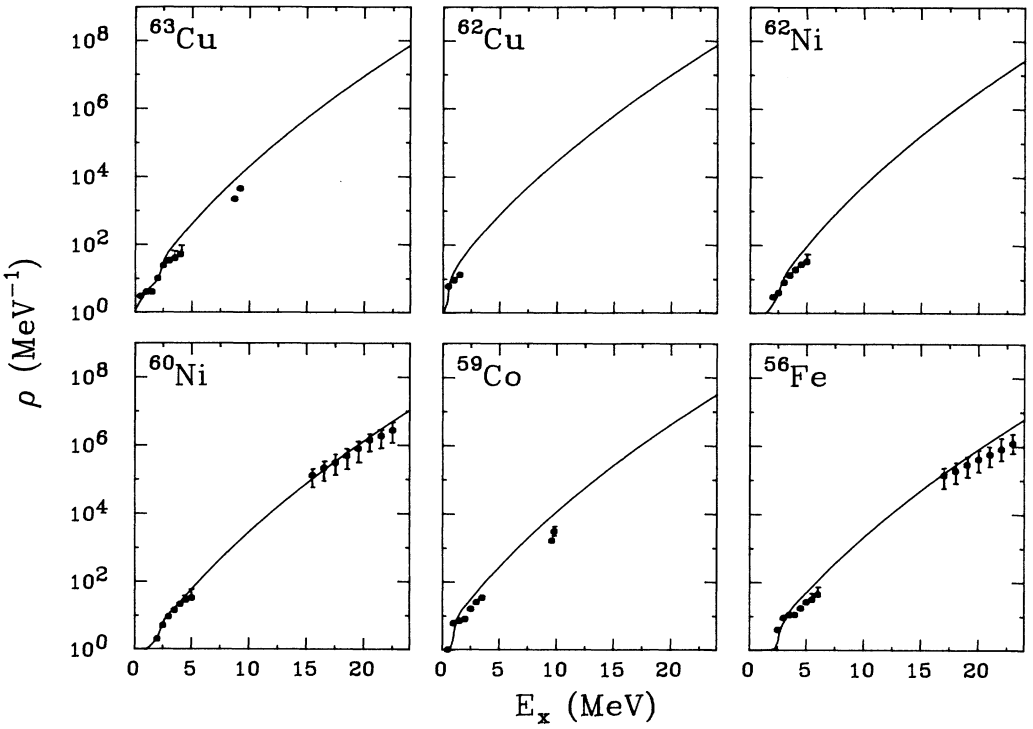

FIG. 8. Level density curves for ^{63}Cu and several daughter nuclei calculated using the Reisdorf approach and the experimental data from Ref. 41.

values of $-(\delta U+\delta P)$ are close to $\Delta_{\rm LDM}$ calculated within the Pühlhofer approach with the Wigner term included. This is because the mass formula[48] used in HIVAP was fitted to experimental masses without the Wigner term included, whereas the mass formula used in the Pühlhofer approach[39] was fitted to data with the Wigner term included. For the damping factor, we used $\gamma^{-1}=18.5$ MeV, as was used in other HIVAP calculations.[47] As pointed out by Schmidt,[45] a damping of the pairing backshift should also be included in order to take into account the pairing interaction for excitation energies below the critical energy ($\sim$5 MeV). However, in our calculations we used the experimentally known individual levels up to $E_x\approx 3.5$ MeV instead. The level density curves calculated with this approach for ^{63}Cu and several daughter nuclei, shown in Fig. 8, agree well with experimental data. Previously, the computer code HIVAP was applied to calculations on much heavier nuclei, and the value of the damping factor $\gamma^{-1}=18.5$ MeV was extracted from data for nuclei with mass $A=100$–253.[44] Schmidt[45] has estimated the damping factor from microscopic calculations to be $\gamma^{-1}=0.4A^{4/3}/\tilde{a}$, which gives $\gamma^{-1}=13$ MeV for ^{63}Cu. In fact, our statistical calculations are completely insensitive to such a change in the factor γ. The GDR parameters extracted from CASCADE fits for these two values of γ are unchanged, except for the GDR strength, which differs by 2%. Therefore, it seems that the Reisdorf formula describes the level density for medium mass nuclei and heavy nuclei equally well. The primary advantage of the latter approach is that it is free of the problems associated with the transition region which are present in the Pühlhofer approach.

The results of CASCADE fits with the level density calculated in the Reisdorf approach are presented in Fig. 9. The best-fit spectral shapes obtained with the Reisdorf approach for the level density reproduce the data significantly better than those shown in Fig. 1. They are essentially identical with fits obtained within the Pühlhofer approach with $a_{\rm LDM}=A/9$ MeV^{-1} and $\Delta_{\rm LDM}$ calculated with the Wigner term included (Fig. 6), and with $a_{\rm LDM}=A/9.5$ MeV^{-1} and $\Delta_{\rm LDM}$ calculated without the Wigner term, and the GDR parameters extracted from fits with those three level density descriptions agree in the range of 5–10%. For example, with the Reisdorf approach, the GDR strength is systematically larger by about 10%, E_D is higher by 2%, and Γ differs typically by 2%, but always by less than 10% when compared with the best fits with the Pühlhofer approach. The extracted GDR parameters combining the results from different level density descriptions are summarized in Table IV (see Sec. III D below)

C. Nonstatistical effects

It has been observed in high-energy γ-ray production in ^{3}He and ^{4}He-induced reactions that large discrepancies occur between statistical calculations and experimental γ-ray spectra. These discrepancies are largest at the highest projectile energies (27 MeV), the highest γ-

ray energies, and for the heaviest target masses.[6,10] Also, the angular distributions of γ rays for these reactions are strongly asymmetrical about $\theta_\gamma = 90°$, showing a large forward-backward asymmetry,[6,10] which is inconsistent with front-back symmetry required by pure statistical decay.

From our best fits using the statistical model, shown in Figs. 6 and 9, there is a small but definite excess of the yield above the calculations at the highest γ-ray energies for ^{4}He+^{59}Co ($E_{\rm lab}[^4{\rm He}] = 28.4$ MeV) and for ^{6}Li+^{57}Fe ($E_{\rm lab}[^6{\rm Li}] = 36.0$ MeV). The discrepancy in the ^{6}Li case is further illustrated in Fig. 2, where one can clearly see that the high-energy γ-ray yield is substantially larger than that observed in ^{18}O+^{45}Sc and in ^{12}C+^{51}V, all forming ^{63}Cu* at the same initial excitation energy $E_{xi} = 52$ MeV. The statistical model describes the ^{12}C and ^{18}O data well at this excitation energy, and it is impossible to adjust the model to fit all three sets of data. A similar conclusion holds regarding the $E_{\rm lab} = 28.4$ MeV ^{4}He data. The fits for these highest-energy ^{6}Li and ^{4}He reactions show the characteristic effects due to a nonstatistical enhancement of the γ-ray yield. Specifically, in addition to the fit discrepancies at high E_γ, the fitted GDR strengths and/or energies are unphysically large (see Table IV). On the other hand, all other spectra are well described by the statistical model fits, with similar GDR parameters for different reactions at similar excitation energies and/or spins. We attribute the observed differences in these ^{4}He and ^{6}Li channels to a nonstatistical enhancement similar to that described in

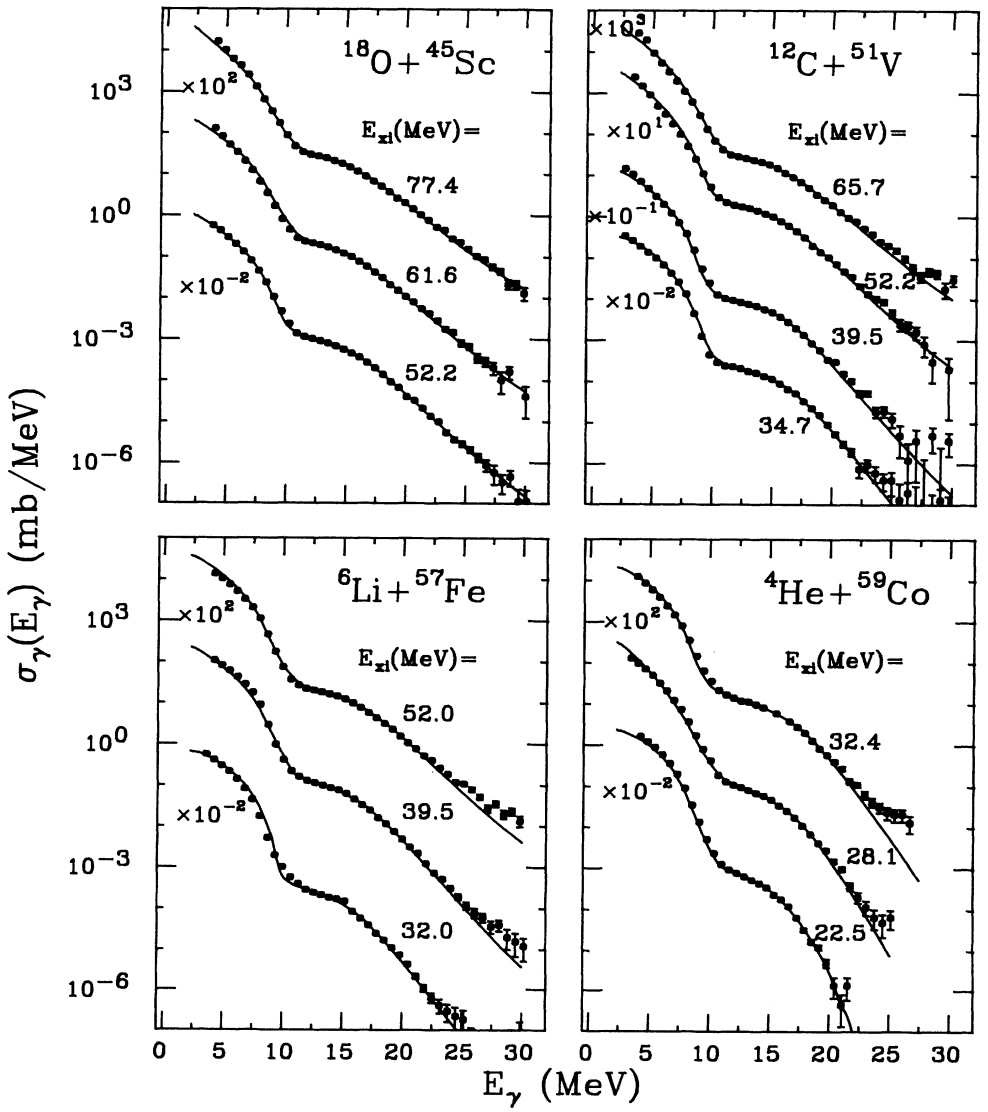

FIG. 9. The same as Figs. 1 and 6, but fitted CASCADE calculations with the Reisdorf level densities.

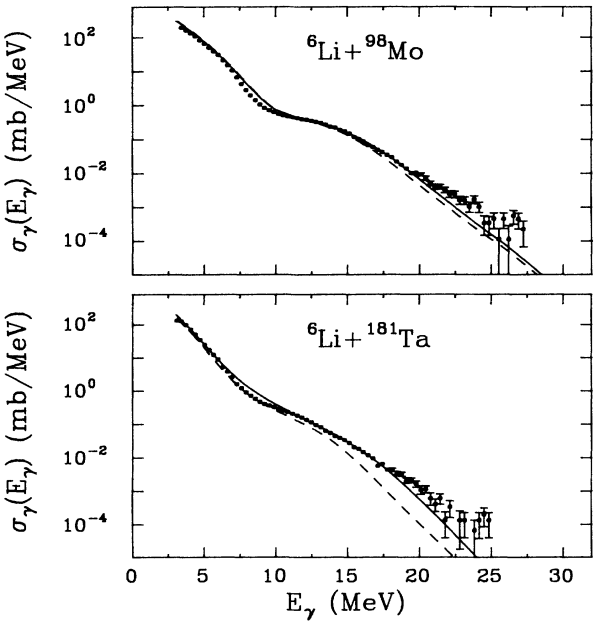

FIG. 10. Meausured γ-ray spectra for the ^{6}Li+^{98}Mo$\rightarrow^{104}$Rh and ^{6}Li+^{181}Ta$\rightarrow^{187}$Os reactions at $E_{\rm lab}[^{6}{\rm Li}]=36.0$ MeV and fitted statistical calculations with level density using the Reisdorf approach (solid lines). The GDR parameters extracted from fits are, for ^{104}Rh*, $S=1.79\pm0.03$, $E_D=16.9\pm0.1$ MeV, and $\Gamma=8.4\pm0.2$ MeV; for ^{187}Os*, $S=5.4\pm0.3$, $E_D=17.9\pm0.3$ MeV, and $\Gamma=10.4\pm0.4$ MeV. Dashed lines show the results of statistical calculations with fixed GDR parameters: for ^{104}Rh* (Ref. 49), $S=1.14$, $E_D=16.15$ MeV, and $\Gamma=8.4$ MeV: for ^{187}Os* (Ref. 50), $S=1.2$, $E_D=14.5$ MeV, and $\Gamma=7.5$ MeV.

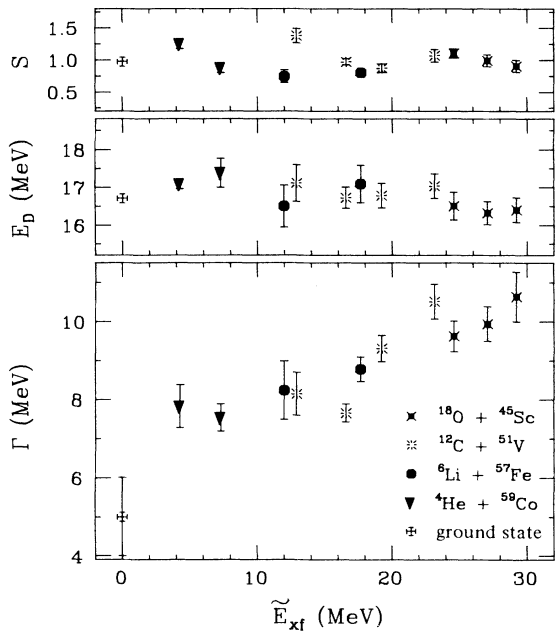

FIG. 11. The extracted GDR parameters of ^{63}Cu as a function of final excitation energy above the yrast line. Ground-state GDR values here and in Figs. 12 and 13 are taken from Refs. 23 and 25 as described in the text.

Refs. 6 and 10.

To explore further the possibility of nonstatistical enhancement of the high-energy γ-ray spectra from ^{6}Li-induced reactions, we have also measured γ rays from ^{6}Li+^{98}Mo and ^{6}Li+^{181}Ta reactions at $E_{\rm lab}[^{6}{\rm Li}]=36.0$ MeV. Comparison between the measured spectra and the fitted CASCADE calculations indicates a strong nonstatistical yield of γ rays above that expected from the statistical model calculations for the ^{6}Li+^{181}Ta reaction and a smaller enhancement for the ^{6}Li+^{98}Mo reaction, as shown in Fig. 10 for calculations with the Reisdorf level density. From the best fits, the apparent GDR strength is in both cases substantially larger then 1.0, and the apparent GDR energy is higher than the ground-state GDR energy. For comparison, we also present in Fig. 10 (dashed lines) CASCADE calculations with reasonable GDR parameters—S and E_D fixed at the values for the GDR built on the ground state,[49,50] and Γ larger by 1 MeV than the ground-state value, as estimated by the excitation energy dependence of Γ in Table IV for ^{63}Cu.

Although the enhancement in the case of ^{6}Li+^{57}Fe appears to be quite small, its effect is observable in the fitted GDR parameters, mainly in a high GDR energy. In Figs. 11–13, we have excluded results from spectra we believe to be contaminated by nonstatistical reaction contributions, namely ^{4}He+^{59}Co ($E_{\rm lab}[^{4}{\rm He}]=28.4$ MeV) and ^{6}Li+^{57}Fe ($E_{\rm lab}[^{6}{\rm Li}]=36.0$ MeV).

D. GDR parameters of ^{63}Cu*

The mean GDR energy, width, and strength (in units of the classical dipole sum rule) which were extracted from the least-squares fits of the CASCADE calculations

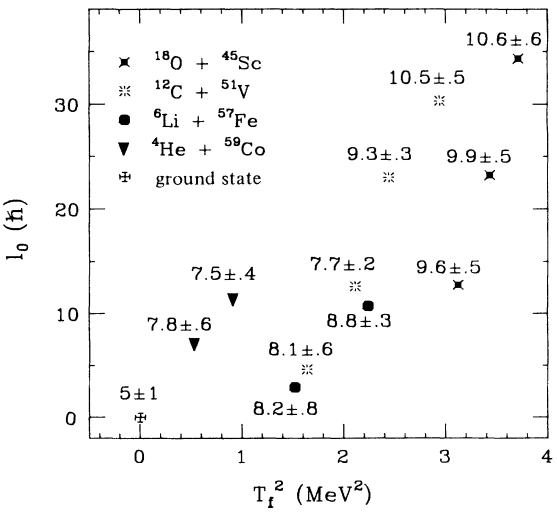

FIG. 12. Two dimensional plot of the extracted width of the GDR of ^{63}Cu as a function of the square of the temperature and the grazing angular momentum l_0.

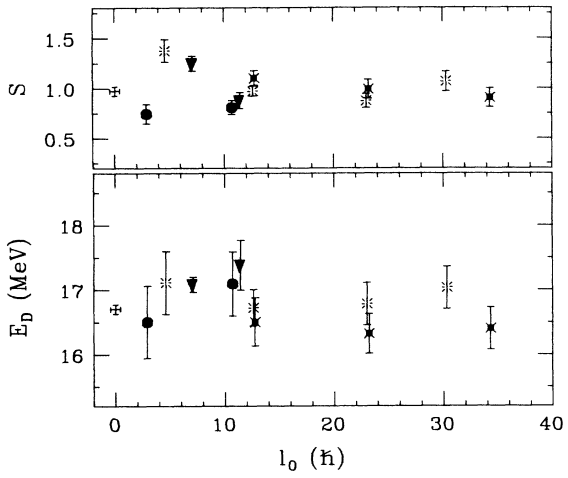

FIG. 13. The strength and energy of the GDR of ^{63}Cu as a function of the grazing angular momentum l_0. See Fig. 12 for identification of symbols.

to the data have been averaged over the different level density descriptions which give good quality fits: (1) the Pühlhofer approach with $a_{\rm LDM}=A/9$ MeV^{-1} and $\Delta_{\rm LDM}$ calculated with the Wigner term, (2) the Pühlhofer approach with a $a_{\rm LDM}=A/9.5$ MeV^{-1} and $\Delta_{\rm LDM}$ calculated without the Wigner term, and (3) the Reisdorf approach with $\gamma^{-1}=18.5$ MeV. Errors in the GDR parameters were calculated as the square root of the sum of squares of the statistical errors given by the fitting procedure and the systematic errors connected with the uncertainty in the level density. Statistical errors are nearly independent of the entrance channel and the excitation energy, and are typically $\Delta S=\pm 0.02$, $\Delta E_D=\pm 0.06$ MeV, and $\Delta\Gamma=\pm 0.2$ MeV.

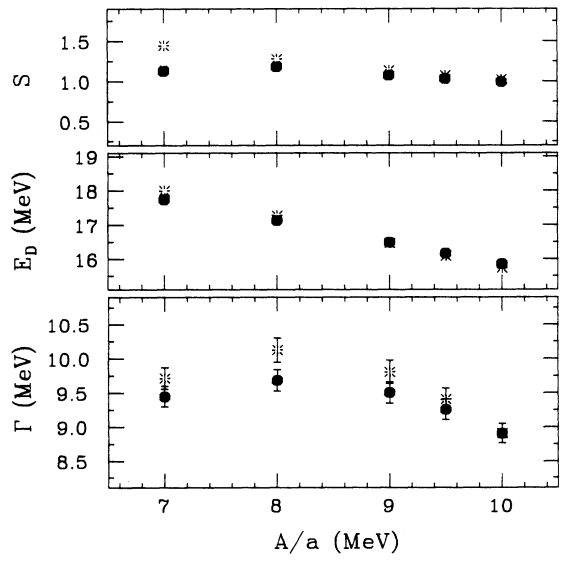

FIG. 14. The level density dependence of the GDR parameters at $E_{xi}=52.2$ MeV in ^{63}Cu formed in the ^{18}O+^{45}Sc reaction channel. Pühlhofer approach was used, with $\Delta_{\rm LDM}$ calculated without the Wigner term (solid dots) and with the Wigner term included (stars).

All the fits presented here were performed with the normal isospin-independent version of CASCADE. Fitted calculations including the effect of isospin using a modified CASCADE code,[51] which are much more time consuming, show that neglecting isospin affects mainly the extracted strength. The strengths obtained for ^{63}Cu* from fits using the isospin-independent code are a factor of $\cong 1.17$ too low compared to a full isospin-dependent calculation. All our quoted strengths have thus been corrected by this factor.

Averaged GDR parameters and errors as discussed above are presented in Table IV and are shown in Fig. 11 as a function of final energy $\tilde{E}_{xf}$ above the yrast line, calculated as $\tilde{E}_{xf}=E_x-E_{\rm rot}-E_D$. E_x is the excitation energy of the decaying nucleus, averaged over the initial compound nucleus and all daughter nuclei that contribute to γ decay with $E_\gamma\cong E_D$. $E_{\rm rot}=I_f(I_f+1)/\theta'$ is the yrast energy calculated for the average final spin I_f. The average final spin I_f was estimated from additional CASCADE calculations in which a weighted average was computed over all decay channels which contribute to γ-ray emission with $E_\gamma=E_D$. The mean initial spin is always equal to or $1\hbar$–$2\hbar$ larger than $2l_0/3$. The mean final spin calculated as described above is always slightly less than the mean initial spin, and within $2\hbar$ of the value of $2l_0/3$. This result implies that in the statistical emission of high-energy γ rays, the spin of the nucleus remains almost unchanged. An important factor in determining this behavior is the high probability for high-energy γ-ray emission at the earliest stages in the decay process.

The final energy $\tilde{E}_{xf}$ is simply related to the mean temperature T_f of states upon which the GDR is built,

$$T_f^2=\tilde{E}_{xf}/a\ ,$$

where a is the level density parameter. To estimate T_f in our analysis, we have used $a=A/8$ MeV^{-1}. The GDR parameters determined as a function of final energy $\tilde{E}_{xf}$ are shown in Fig. 11. It appears that in the range of temperatures studied the strength and resonance energy of the GDR built on highly excited states do not depend on excitation energy or, equivalently, temperature, and are close to their ground-state values (see Fig. 11). The GDR width increases smoothly with increasing excitation energy, and the basic character of this dependence is not affected by changes in the level density parameters.

For a given nuclear reaction, higher bombarding energies generally correspond to higher spins as well as higher compound nuclear temperatures. To show how the width of the GDR depends separately on the spin and the temperature, a two-dimensional plot of the GDR width as a function of temperature and grazing angular momentum l_0 is presented in Fig. 12. It can be seen that the broadening of the GDR is connected both with an increase in spin and with an increase in temperature, but that the temperature dependence is dominant.

The GDR energy and strength were shown not to depend on nuclear temperature (Fig. 11). In Fig. 13 these

quantities are presented as a function of angular momentum. Apparently, there is no systematic spin dependence of the energy and strength of the GDR. This result differs from the case reported by Schwalm *et al.*[52] who have observed a systematic decrease of the GDR energy in Er isotopes with spin increasing from $5\hbar$ to $50\hbar$.

As we have shown, the CASCADE calculations are sensitive to the level density parameters. To show how changes in the level density parameters of the "high" energy region affect the GDR parameters, the dependence of the latter as a function of a_{LDM} using the Pühlhofer approach for two values of Δ_{LDM} (calculated with and without the Wigner term) are presented for an initial excitation energy of $E_{xi}=52.2$ MeV in Fig. 14. The character of this dependence is similar for higher initial excitation energies, and is even stronger for lower energies, due to the role of the transition region. Upper and lower limits on possible values of a_{LDM} for the range of masses studied are determined by the quality of the fits, which deteriorate for a_{LDM} outside the range of $A/9.5$ $\mathrm{MeV}^{-1} \leq a_{\mathrm{LDM}} \leq A/8$ MeV^{-1}. Within those limits the energy of the GDR built on highly excited states remains unchanged within ± 0.5 MeV compared to the ground-state value, in agreement with theoretical predictions.[12,14,20] In the Reisdorf level density approach, which gives good fits to the data, there is no freedom to arbitrarily change the parameter $\tilde{a}$. Changes of the damping factor γ^{-1} in a reasonable range (10–20 MeV) affect the energy-dependent a, but do not affect the shape of the γ-decay spectra or the fitted GDR parameters.

IV. SUMMARY AND CONCLUSION

The analysis presented here of the statistical GDR decay as a function of temperature and spin in ^{63}Cu* is the most detailed experimental study of the GDR parameters in a given nucleus presently available.

We have found that the GDR parameters for the same initial excitation energy produced by the $^{18}\mathrm{O}+^{45}\mathrm{Sc}$ and $^{12}\mathrm{C}+^{51}\mathrm{V}$ entrance channels are very similar, indicating, at most, a weak spin dependence. The mean GDR energy of $E_D=16.8\pm0.4$ MeV at finite temperature observed in the present work is in agreement with the average ground-state $T_<$ value of $E_{\mathrm{g.s.}}=16.7$ MeV discussed in Sec. I. Furthermore, the average strength of $S=0.99\pm0.10$ is in agreement with $S_{\mathrm{g.s.}}=0.97$.[21] The width varies smoothly from 7.5 ± 0.4 to 10.6 ± 0.6 MeV in the temperature range from 0.7 to 1.9 MeV. These widths may be compared with $\Gamma_{\mathrm{g.s.}}\cong 5\pm1$ MeV for the $T_<$ component of the ground-state GDR estimated from results for ^{60}Ni.[29]

These results are consistent with theoretical expectations that the GDR strength and energy should not change as a function of temperature and spin in the range of this work, while the width should broaden at higher temperature due to thermal averaging over a distribution of deformations.[19] The temperature dependence of the GDR width in ^{63}Cu* is similar to the experimental evidence for broadening of the GDR in ^{108}Sn* and ^{111}Sn*.[11]

In contrast to heavier nuclei, which often require a two-component GDR strength function, all of the data presented here are well fitted by statistical model calculations with a one-component GDR (except for the highest-energy ^{4}He and ^{6}Li data, which show a nonstatistical enhancement).

An additional conclusion of the present statistical analysis is the suggestion that for nuclei with $A\approx 60$ the level density can be determined using the Pühlhofer approach, either with the parameters $a_{\mathrm{LDM}}=a/9$ MeV^{-1} and Δ_{LDM} calculated including the Wigner term, or $a_{\mathrm{LDM}}=A/9.5$ MeV^{-1} and Δ_{LDM} calculated without the Wigner term. Alternatively, the Reisdorf approach with $\gamma^{-1}=18.5$ MeV can be used. The Reisdorf approach with the inclusion of individual levels at low excitation energy seems to be more reliable, as it is free from uncertainties in the "high" energy level density parameters and in the transition region description.

ACKNOWLEDGMENTS

Two of us (M.K.-H. and E.F.G.) would like to thank the University of Washington for financial support and the members of the University of Washington Nuclear Physics Laboratory for their generous hospitality. We are indebted to Dr. C.C. Sahm (GSI, Darmstadt) for kindly providing us with the computer code HIVAP.

*Permanent address: Institute of Experimental Physics, University of Warsaw, 00681 Warsaw, Poland.

[1]J. O. Newton, B. Herskind, R. M. Diamond, E. L. Dines, J. E. Draper, K. H. Lindenberger, C. Schuck, S. Shih, and F. S. Stephens, Phys. Lett. **46**, 1383 (1981).

[2]J. E. Draper, J. O. Newton, L. G. Sobotka, H. Lindenberger, G. J. Wozniak, L. G. Moretto, F. S. Stephens, R. M. Diamond, and R. J. McDonald, Phys. Rev. Lett. **49**, 434 (1982).

[3]A. M. Sandorfi, J. Barrette, M. T. Collins, D. H. Hoffmann, A. J. Kreiner, D. Branford, S. G. Steadman, and J. Wiggins, Phys. Lett. **130B**, 19 (1983).

[4]W. Hennerici, V. Metag, H. J. Hennrich, R. Repnow, W. Wahl, D. Habs, K. Helmer, U. V. Helmolt, H. W. Heyng, B. Kolb, D. Pelte, D. Schwalm, R. S. Simon, and R. Albrecht, Nucl. Phys. **A396**, 329c (1983).

[5]E. F. Garman, K. A. Snover, S. H. Chew, S. K. B. Hesmondhalgh, W. N. Catford, and P. M. Walker, Phys. Rev. C **28**, 2554 (1983).

[6]K. A. Snover, Comments on Nucl. Part. Phys. **12**, 243 (1984); J. Phys. (Paris) Colloq. **45**, C4-337 (1984); in *Capture Gamma-Ray Spectroscopy and Related Topics—1984 (International Symposium, Knoxville, Tennessee)*, AIP Conf. Proc. No. 125, edited by S. Raman (AIP, New York, 1985), p. 660.

[7]J. J. Gaardhøje, O. Andersen, R. M. Diamond, C. Ellegaard, L. Grodzins, B. Herskind, Z. Sujkowski, and P. M. Walker, Phys. Lett. **139B**, 273 (1984).

[8]J. J. Gaardhøje, C. Ellegaard, B. Herskind, and S. G. Steadman, Phys. Rev. Lett. **53**, 148 (1984).
[9]C. A. Gossett, K. A. Snover, J. A. Behr, G. Feldman, and J. L. Osborne, Phys. Rev. Lett. **54**, 1486 (1985).
[10]K. A. Snover, Annu. Rev. Nucl. Part. Sci. **36**, 545 (1986).
[11]J. J. Gaardhøje, C. Ellegaard, B. Herskind, R. M. Diamond, M. A. Deleplanque, G. Dines, A. O. Macchiavelli, and F. S. Stephens, Phys. Rev. Lett. **56**, 1783 (1986).
[12]H. M. Sommermann, Ann. Phys. (N.Y.) **151**, 163 (1983).
[13]M. E. Faber, J. L. Egido, and P. Ring, Phys. Lett. **127B**, 5 (1983).
[14]P. Ring, L. M. Robledo, J. L. Egido, and M. Faber, Nucl. Phys. **A419**, 261 (1984).
[15]D. Vautherin and N. Vinh Mau, Nucl. Phys. **A422**, 140 (1984).
[16]O. Civitarese, R. A. Broglia, and C. H. Dasso, Ann. Phys. (N.Y.) **156**, 142 (1984).
[17]H. Sagawa and G. F. Bertsch, Phys. Lett. **146B**, 138 (1984).
[18]J. Bar-Touv, Phys. Rev. C **32**, 1369 (1985).
[19]M. Gallardo, M. Diebel, T. Døssing, and R. A. Broglia, Nucl. Phys. **A443**, 415 (1985).
[20]S. Yang and Z. Szymanski, Nucl. Phys. **A436**, 397 (1985).
[21]S. C. Fultz, R. L. Bramblett, J. T. Caldwell, and R. R. Harvey, Phys. Rev. **133**, B1149 (1964).
[22]D. G. Owen, E. G. Muirhead, and B. M. Spicer, Nucl. Phys. **A122**, 177 (1968).
[23]R. E. Sund, M. P. Baker, L. A. Kull, and R. B. Walton, Phys. Rev. **176**, 1366 (1968).
[24]F. Dreyer, H. Dahmen J. Staude, and H. H. Thies, Nucl. Phys. **A181**, 477 (1972).
[25]B. L. Berman and S. C. Fultz, Rev. Mod. Phys. **47**, 713 (1975).
[26]P. Paul, J. F. Amann, and K. A. Snover, Phys. Rev. Lett. **27**, 1013 (1971).
[27]P. Carlos, H. Beil, R. Bergere, J. Fagot, A. Lepretre, and A. Veyssiere, Nucl. Phys. **A258**, 365 (1976).
[28]E. M. Diener, J. F. Amann, and P. Paul, Phys. Rev. C **3**, 2303 (1971).
[29]T. J. Bowles, R. J. Holt, H. E. Jackson, R. D. McKeown, A. M. Nathan, and J. R. Specht, Phys. Rev. Lett. **48**, 986 (1982).
[30]R. O. Akyuz and S. Fallieros, Phys. Rev. Lett. **27**, 1016 (1971).
[31]S. Fallieros and B. Goulard, Nucl. Phys. **A147**, 593 (1970).
[32]N. V. Lin Kova, R. M. Osokina, B. S. Ratner, R. Sh. Amirov, and V. V. Akindinov, Zh. Eksp. Teor. Fiz. **38**, 78 (1960).
[33]M. Hasinoff, S. T. Lim, D. F. Measday, and T. J. Mulligan, Nucl. Instrum. Methods **117**, 375 (1974).
[34]D. H. Dowell, C. A. Gossett, and K. A. Snover, University of Washington, Nuclear Physics Laboratory Annual Report, 1984, p. 78.
[35]F. Pühlhofer, Nucl. Phys. **A280**, 267 (1977).
[36]Y. Kawazoe, H. Miyase, H. Tsubota, J. Yokokawa, M. Oyamada, and Y. Torizuka, Phys. Rev. C **33**, 1917 (1986).
[37]IAEA Advisory Group Meeting on Basic and Applied Problems of Nuclear Level Densities, June, 1983, edited by M. R. Bhat, National Nuclear Data Center, Brookhaven National Laboratory (unpublished).
[38]W. Dilg, W. Schantl, H. Vonach, and M. Uhl, Nucl. Phys. **A217**, 269 (1973).
[39]W. D. Myers, *Droplet Model of Atomic Nuclei* (IFI/Plenum, New York, 1977).
[40]W. D. Myers, Nucl. Phys. **A204**, 465 (1973).
[41]C. C. Lu, L. C. Vaz, and J. R. Huizenga, Nucl. Phys. **A190**, 229 (1972).
[42]S. Gil, R. Vandenbosch, A. J. Lazzarini, D.-K. Lock, and A. Ray, Phys. Rev. C **31**, 1752 (1985).
[43]A. V. Ignatyuk, G. N. Smirenkin, and A. S. Tishin, Yad. Fiz. **21**, 485 (1975) [Sov. J. Nucl. Phys. **21**, **255**, (1975)].
[44]W. Reisdorf, Z. Phys. A **300**, 227 (1981).
[45]K. H. Schmidt, H. Delagrange, J. P. Dufour, N. Carjan, and A. Fleury, Z. Phys. A **308**, 215 (1982).
[46]S. K. Kataria, V. S. Ramamurthy, and S. S. Kapoor, Phys. Rev. C **18**, 549 (1978).
[47]D. Vermeulen, H. G. Clerc, C. C. Sahm, K. H. Schmidt, J. G. Keller, G. Münzenberg, and W. Reisdorf, Z. Phys. A **318**, 157 (1984); C. C. Sahm, H. G. Clerc, K. H. Schmidt, W. Reisdorf, P. Armbruster, F. P. Hesseberger, J. G. Keller, G. Münzenberg, and D. Vermeulen, Nucl. Phys. **A441**, 316 (1985).
[48]W. D. Myers and W. J. Swiatecki, Ark. Fys. **36**, 343 (1967).
[49]A. Lepretre, H. Beil, R. Bergere, P. Carlos, A. de Miniac, A. Veyssiere, and K. Kernbach, Nucl. Phys. **A219**, 39 (1974).
[50]B. L. Berman, D. D. Faul, R. A. Alvarez, P. Meyer, and D. L. Olson, Phys. Rev. C **19**, 1205 (1979).
[51]M. N. Harakeh, D. H. Dowell, G. Feldman, E. F. Garman, R. Loveman, J. L. Osborne, and K. A. Snover, Phys. Lett. **176B**, 297 (1986).
[52]D. Schwalm, Ch. Ender, H. Groger, D. Habs, U. V. Helmolt, W. Hennerici, H. J. Hennerich, H. W. Heyng, W. Korten, R. Kroth, M. Music, J. Schrimer, B. Schwartz, W. Wahl, R. S. Simon, W. Kühn, V. Metag, and C. Broude, Max-Planck-Institut für Kernphysik Report MPI H-1984-V35, 1984.